Electronic Supplementary Material (ESI) for New Journal of Chemistry.

# Electronic Supporting Information (ESI)

# Supramolecular "All-in-one" Nanodrug Based on Perylene Diimide for Dual-mode Imagings Guided PTT-chemotherapy

Jiazhen Wu,[a] Nan Wang,[b] Guozheng Liu,[a] Mingming Luan,[a] Mingyang Zhou,[a] and Yanjuan Wu*[a]

[a] School of Chemistry and Chemical Engineering, Qilu University of Technology (Shandong Academy of Sciences), Jinan 250353, PR China

[b] Henan University of Chinese Medicine, Zhengzhou 450000, PR China

*E-mail: wuyanjuan5@qlu.edu.cn;

# Table of Contents

1. Materials

2. Instruments

3. Experiments

4. Scheme and Figures

Scheme S1. Schematic illustration of the synthesis of PDI0.

Fig. S1 (A) $^{1}$H NMR spectrum of HOOC-PDI-COOH in DMSO-$d_6$. (B) $^{1}$H NMR spectrum of PDI0 in DMSO-$d_6$. (C) MS spectrum of PDI0 in acetonitrile (chromatographically pure).

Fig. S2 FT-IR spectra of free drugs (DOX, PDI0) and prepared DP NPs.

Fig. S3 Tyndall effect of DP1 and DP3.

Fig. S4 (A) Fluorescence spectra of free DOX and DP NPs in deionized water. (B) Fluorescence spectra of free PDI0 and DP NPs in deionized water.

Fig. S5 The standard curves of PDI0 (A) and DOX (B) in DMSO.

Fig. S6 DLS (A) and TEM (B) of free PDI0; DLS (C) and TEM (D) of free DOX.

Fig. S7 The hydrodynamic diameter of DP1 (A) and DP3 (B) in pH 5.0.

Fig. S8 Zeta potential measurement of DP2 in PBS (pH 7.4) (A) and in PBS (pH 5.0) (B).

Fig. S9 (A) $N_2$ adsorption – desorption isotherms of DP2, (B) XPS spectrum of DP2, (C) TGA thermograms.

Fig. S10 Photographs and Tyndall effect of DP2 at different concentrations.

Fig. S11 (A) Photothermal effect of free PDI0 at different concentrations with 660 nm laser irradiation (1 W/cm$^2$). (B) Photothermal heating curves of free PDI0 (30 μg/mL) under different laser power densities. (C) Photothermal heating and cooling curves of water. (D) The relationship of negative natural logarithm of θ and cooling time of water.

Fig. S12 The infrared thermal images of DP2 (40 μg/mL) irradiated with 660 nm laser under different power densities.

Fig. S13 Photographs of PDI0 under different pH, (A) 7.4 and (B) 5.0.

Fig. S14 (A) CLSM images of HepG 2 cells incubated with free DOX and DP2 for 0.5, 2 and 4 h (scale bar: 25 μm). (B) Flow cytometry (FCM) analysis of HepG 2 cells after incubation with free DOX and DP2.

Fig. S15 CLSM images of HeLa and HepG 2 cells incubated with DP2 in the presence or absence of 660 nm laser for 2 h (scale bar: 25 μm).

Fig. S16 Cell viability of HepG 2 cells incubated with DOX, DOX + Laser, PDI0, PDI0 + Laser, DP2, and DP2 + Laser at different concentrations for 24 h (A) and 48 h (B).

Fig. S17 The photothermal images of 4T1 tumor-bearing mice after injection of PBS.

Fig. S18 Photograph of 4T1 tumors harvested at day 14 after different treatments.

Fig. S19 H&E staining of heart, liver, spleen, lung and kidney from different treatment groups (Scale bar: 100 μm).

## 1. Materials

Doxorubicin hydrochloride (DOX, 98%), 6-aminocaproic acid (98%) were obtained from Anergy Chemical Reagent (Shanghai, China). 1,7-dibromo-3,4,9,10-tetracarboxylc acid dianhydride (95%) was purchased from Alfa Chemical Co., Ltd. (Zhengzhou, China). Tetrahydropyrrole (99%) and propionic acid (99.5%) were obtained from Aladdin Chemical Co., Ltd. (Shanghai, China). Phosphate-buffered saline (PBS), high-glucose medium (DMEM), fetal bovine serum (FBS), pen-strep solution (penicillin: 100 U/mL, streptomycin: 0.1 mg/mL) and trypsin EDTA solution were bought from Biological Industries (Shanghai, China). Antifade mounting medium with DAPI and methylthiazolyldiphenyl-tetrazolium bromide (MTT, 98%) were obtained from Beyotime Biotech. Inc. (Shanghai, China). Sodium phosphate monobasic dihydrate ($NaH_2PO_4 \cdot 2H_2O$, AR) and 1-methyl-2-pyrrolidinone (NMP, 99%) were obtained from Maclin Reagent (Shanghai, China). Disodium hydrogen phosphate dodecahydrate ($Na_2HPO_4 \cdot 12H_2O$, AR), acetic acid (AR), dichloromethane (DCM, AR), methanol (AR) and dimethyl sulfoxide (DMSO, AR) were purchased from Sinopharm Group Chemical Reagents Co., Ltd (Shanghai, China).

## 2. Instruments

$^1H$ NMR spectrum was obtained using an AVANCE II 400 MHz NMR spectrometer (Bruker) using DMSO-*d6* as solvent at room temperature. The Fourier Transform Infrared (FT-IR) spectra were obtained by NEXUS 670 Fourier spectrometer (Nicolet, USA). The UV-Vis absorption spectra and fluorescence spectra were measured on the UV–Vis spectrophotometer (Metash, UV-8000) and F97Pro fluorescent spectrophotometer (Shanghai, China), respectively. The size, size distribution and zeta potential nanodrugs were measured by the Laser Particle Size Analyzer Zetasizer (Malvern Nano-ZS 90). The size and morphology of the constructed nanodrugs were observed by a JEM-2100 Transmission Electron Microscope (TEM) (JEOL, Japan). Confocal laser scanning microscopy (CLSM) images were accomplished with a Leica SP8 confocal laser scanning microscopy (Germany). Flow cytometry was used to quantitatively determine the fluorescence intensity of cells, measured on a CytoFLEX Flow cytometer (Beckman Coulter, China). MTT analysis was performed using a

Synergy Neo2 microplate reader. The 660 nm infrared laser (Xi'an Reaser Electronic Technology Co., Ltd.) was used to measure the photothermal performance of the prepared nanodrugs. Drug release assays were performed when incubated with a SHA-B oscillator. The photothermal images were taken by a FLIR pro thermal camera. The surface area was measured by using a Autosorb-iQ system. X-ray photoelectron spectroscopy (XPS) was performed using the Thermo Scientific ESCALAB Xi+ systems to analyze the near surface region elemental composition of DP2. Thermal stability of DOX, PDI0 and DP2 were studied by using METTLER TOLEDO TGA-2.

**3. Experiments**

**Synthesis of PDI0**

First, 25 mL of DMP was completely mixed with propionic acid (8 mL). 1,7-dibromo-3,4,9,10-tetracarboxylc acid dianhydride (2.00 g, 3.635 mmol) and 6-aminocaproic acid (2.86 g, 21.811 mmol) were added into the above mixed solvent. The reaction was protected with $N_2$, and stirred at 85 ℃ for 36 h in the dark. After cooling to 20 ℃, solution was poured into deionized water (500 mL). Then the crude product was filtered and dried. Silica gel column chromatography was applied to purify the product by using dichloromethane/acetic acid 80/1 as the solvent system, yielding 2.26 g of red powder, named as HOOC-PDI-COOH.

Next, a mixture of HOOC-PDI-COOH (2.00 g, 2.58 mmol) and tetrahydropyrrole (30 mL) was stirred under the protection of $N_2$ for 36 hours at 60 ℃ in the dark. Then, the solution was dried to remove the superfluous tetrahydropyrrole. Silica gel column chromatography was conducted to purify the solid by using dichloromethane/methanol 40/1 as the solvent system, yielding 1.08 g of green powder (named as PDI0).

**Preparation of supramolecular nanodrugs (DP NPs)**

The carrier-free supramolecular nanodrugs (DP NPs) were prepared by a simple co-assembly approach between two small molecules drugs (PDI0 and DOX). In brief, DMSO was used to dissolve PDI0 to prepare stock solution with a concentration of 10 mg/mL, while DOX·HCl (10 mg) was dissolved in deionized water (1 mL). Afterward,

200 μL of DOX and 200 μL of PDI0 were injected into deionized water (4 mL) simultaneously under ultrasound. Subsequently, suspension was gently stirred at room temperature for 2 hours in dark environment. And then, a dialysis bag (MWCO: 3.5 kDa) was used to install the mixture. After dialyzing for 24 hours, dialysate was lyophilized to obtain nanodrug with the feed mass ratio of 1:1 (named as DP2). Other nanoformulations were constructed in a similar way except for changing the feed mass ratios of PDI0 to DOX (5:3 and 3:5).

**Drug loading capacity**

3 mg of freeze-dried DP NPs was dissolved DMSO (30 mL) in the dark. To measure the DOX and PDI0 content, UV−Vis spectrometer was used to character the prepared solution. The DOX/PDI0 loading content (DLC) was calculated according to the formula as follow:

DLC (%) = [(mass of DOX/PDI0 in DP NPs) / (total mass of DP NPs) × 100%]

**Stability evaluation of DP2**

Initially, DLS measurements were determined to investigate the stability property. To study the pH effect, DP2 (3 mg) were suspended in PBS 7.4 (6 mL) and PBS 5.0 (6 mL), respectively. Subsequently, DLS measurement was proceeded at predetermined time point to determine the size and size distribution. Then, DP2 (3 mg) were dispersed in PBS 7.4 (6 mL), and irradiated by 660 nm laser (1 W/cm$^2$) for 30, 120, and 300 s, respectively. DLS measurement was also conducted to characterize the light responsiveness. Furthermore, the light responsiveness of the prepared DP2 was researched by using UV-Vis absorption spectrum. DP2 in PBS 7.4 (0.5 mg/mL) was irradiated by 660 nm laser (1 W/cm$^2$), and UV-Vis absorption spectra were recorded every minute.

**Photothermal properties of DP2**

The photothermal conversion capacity of DP2 was carefully evaluated using a 660 nm laser and a digital thermometer. For this purpose, DP2 was dispersed in deionized water at 0, 10, 20, 40 and 60 μg/mL, and irradiated with 660 nm laser (1 W/cm$^2$) for 300 s respectively. The temperature variation of the samples was

recorded by a digital thermometer every 10 s. To study the influence of laser power intensity on photothermal conversion capacity, DP2 (30 μg/mL) in deionized water were irradiated with 660 nm laser (0.5, 0.8, 1.0, 1.2, and 1.5 W/cm$^2$) for 300 s respectively. Then, the temperature variation was also monitored. Furthermore, the photostability of DP2 was explored. DP2 (30 μg/mL) in deionized water were continuously exposed to 660 nm laser (1 W/cm$^2$) for 300 s. After shutting off the laser, the mixture was cooled down naturally. The on/off cycle irradiation tests were carried out for 5 cycles. The photothermal conversion efficiency (η) was obtained according to the literature.[1]

***In vitro* drug release**

To determine the *in vitro* drugs release profile of DP2, a dialysis method was employed. In general, DP2 (3 mg) was redispersed in PBS (4 mL) with a pH of 7.4 or 5.0. The samples were then sealed in dialysis bags (MWCO=3.5 kDa), and immersed in corresponding buffer solution (36 mL). Subsequently, the mixture was put in an oscillator at 37 ℃ in the dark. Moreover, to evaluate the effect of laser irradiation, at 1, 3, and 7 h, the mixture was exposed to 660 nm laser (1 W/cm$^2$) for 300 s. At predetermined time intervals, the supernatant (3 mL) was collected, and replaced with corresponding fresh buffer (3 mL). The amount of released PDI0 was evaluated using the UV−Vis absorption spectra, and the release efficiency of DOX was measured by a fluorescence spectrometer with excitation at 485 nm and emission at 595 nm.

***In vitro* imagings**

To investigate the photothermal imaging ability, DP2 (60, 40, 20, 10 and 0 μg/mL of PDI0) in deionized water were injected into EP tubes and irradiated with 660 nm laser (1 W/cm$^2$) for 5 min respectively. The photothermal imagings were recorded by a FLIR pro thermal camera every minute. In addition, DP2 (60, 40, 20, 10 and 0 μg/mL of PDI0) aqueous solution in EP tubes was irradiated with 660 nm laser (0.5, 0.8, 1.0, 1.2, 1.5 W/cm$^2$) for 300 s respectively, then the photothermal imagings were also conducted.

The *in vitro* photoacoustic (PA) imaging ability of DP2 was studied by using a

photoacoustic imaging system (Vevo LAZR, Visual Sonics Inc., Canada). First, the full PA spectrum of DP2 was collected. 300 μL of DP2 aqueous solution (0.2 mg/mL) was injected into the sample cell, and scanned by PA imaging system with the excitation wavelengths from 680 to 970 nm. Then, to evaluate the concentration effect, PA signal intensities of different concentrations of DP2 (0.03 to 0.1 mg/mL) were determined by the region of interest (ROI) analysis with the excitation wavelengths of 690 nm.

**Cell culture**

The hepatocellular carcinoma cells (HepG 2) and human cervical cancer cells (HeLa) were provided by the Institute of Biochemistry and Cell Biology, Chinese Academy of Sciences (Shanghai, China). All cells were incubated in DMEM medium supplemented with 1% antibiotics (100 U/mL penicillin and 100 U/mL streptomycin) and 10% FBS in a humidified incubator at 37 ℃ with 5% $CO_2$.

***In vitro* intracellular uptake and intracellular distribution**

In brief, a total of $1 \times 10^6$ cancer cells were seeded in a 6-well plate. After incubating for 18 h, the medium was deserted and replaced by fresh DMEM solutions containing free DOX (10 μg/mL) or DP2 (DOX: 10 μg/mL). After cultured for another 0.5, 2 or 4 h, the culture medium was removed. The cold PBS was used for washing. The cells were fixed with 4% paraformaldehyde in PBS for 20 min, and rinsed with cold PBS for three times. Then the cells were stained with DAPI, and observed by CLSM. To evaluate the effect of laser irradiation, HeLa/HepG 2 cells were cultured in a 6-well plate at $1 \times 10^6$ cells/well for 24 h. Then, the cells were treated with DP2 containing 10 μg/mL of DOX. After 2 h incubation, the cells were irradiated by a 660 nm laser at 0.8 W/$cm^2$ for 10 min. Then, the cells were washed and fixed. Finally, the cells were stained with DAPI for CLSM observation. In addition, cells without laser treatment were used as control. Simultaneously, flow cytometry was used to quantitatively determine the fluorescence intensity of cells. $1 \times 10^6$ cancer cells

were seeded in a 12-well plate and incubated overnight. Then the medium was replaced with fresh DMEM solutions which contains free DOX (10 μg/mL) or DP2 (DOX: 10 μg/mL). After cultured for another 0.5, 2 or 4 h, the cells were rinsed with cold PBS, trypsinized, and gathered for flow cytometer analysis.

***In vitro* cytotoxicity**

The cytotoxicity of free DOX, PDI0 and DP2 against HeLa and HepG 2 cells with or without laser treatment was evaluated by methyl thiazolyl tetrazolium (MTT) assay. Tumor cells were seeded into 96-well plates ($3 \times 10^4$ cells/well). After culturing for another 24 h, fresh medium containing serial concentrations of free DOX, PDI0 or DP2 were added into the wells, respectively. After incubatiing in the dark for 6 h, the light irradiation groups were exposed to 660 nm laser (0.8 W/cm$^2$) for 300 s, and cultured for another 18 h or 42 h. Then, 15 μL of MTT (5 mg/mL) were added to each well, and the cells were incubated for another 4 h at 37 ℃ in the dark. Finally, the MTT-containing media were replaced by 150 μL of DMSO, and the absorbance was measured on a Synergy Neo2 microplate reader.

**Animal model**

All animal experiments were in according with the animal protocols approved by the Institutional Animal Care and Use Committee of Fuzhou University. Female BALB/c mice (aged 5 to 6 weeks) were obtained from Shanghai SLAC laboratory Animal Co., Ltd. To obtain 4T1 tumor-bearing mice, 4T1 cells ($2 \times 10^6$) suspended in 50 μL PBS were subcutaneously injected into the left hind leg of each mouse. The tumor volume (V) was calculated as $V = \text{width}^2 \times \text{length}/2$.

***In vivo* photothermal and PA imaging**

The 4T1 tumor-bearing mice were used to investigate the *in vivo* photothermal imaging ability. The mice were injected with DP2 (3 mg/mL, 100 μL) via the tail vein. After 24 h intravenous injection, the tumor region was treated with a 660 nm (0.8 W/cm$^2$). The photothermal imagings were also recorded by a FLIR pro thermal camera every minute.

For *in vivo* PA imaging, the 4T1 tumor-bearing mice were administrated with DP2 (3 mg/mL, 100 μL) via the tail vein. At the post-injection time of 2, 8, 14, and 24 h, mice were anesthetized, and the tumor region was imaged by the photoacoustic imaging system (Vevo LAZR, Visual Sonics Inc., Canada) at room temperature, the peak absorption of DP2 at 690 nm was fixed as excitation wavelength.

***In vivo* antitumor activity**

When the tumor volume reached about 60-150 $mm^3$, the 4T1 tumor-bearing mice were randomly divided into 6 groups (n=4, each group). The mice were received the following treatments: 1) treated with PBS; 2) treated with DOX (3 mg/kg); 3) treated with PDI0 (3 mg/kg); 4) treated with DP2 (3 mg/kg of DOX); 5) treated with PDI0 (3 mg/kg) plus 660 nm laser; 6) treated with DP2 (3 mg/kg of DOX) plus 660 nm laser. All the drugs were injected with the tail vein, and treatments were performed at 0, 3 and 6 day. For group 5 and 6, 24 h post intravenous injection, the tumor sites were irradiated by a 660 nm laser (0.5 $W/cm^2$) for 5 min. The tumor size was measured by caliper, the tumor volume and body weight were recorded every two days. A total of 14 days later, the mice were sacrificed. The tumors and main tissues were harvested for hematoxylin-eosin (H&E) staining.

**Statistical Analysis.**

Data are represented as the mean values ± standard deviation (mean ± SD). The data were analyzed using GraphPad Prism 6. The t test was used to test for significant differences.

## 4. Scheme and Figures

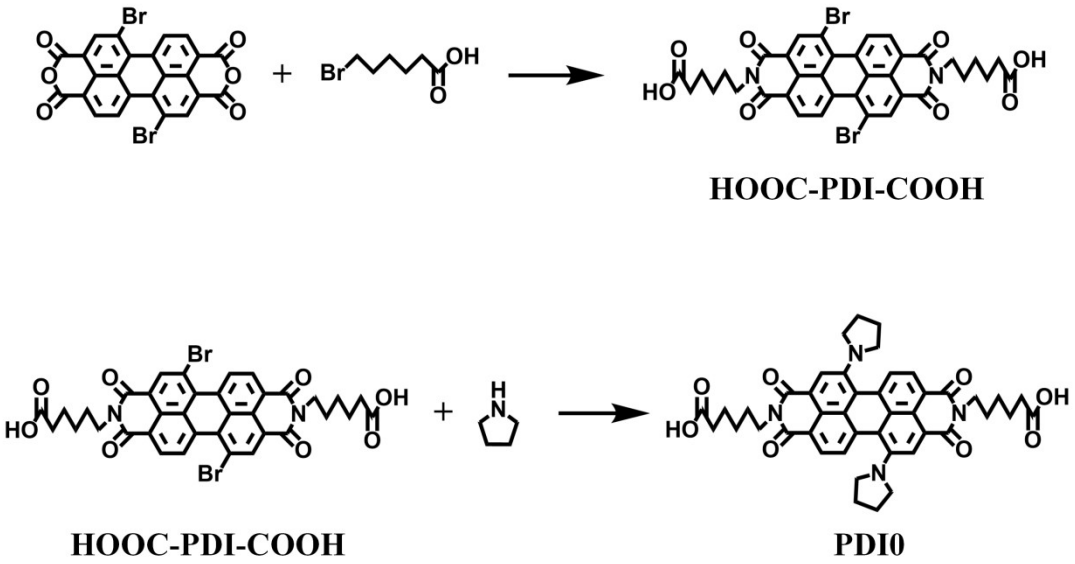


**Scheme S1.** Schematic illustration of the synthesis of PDI0.

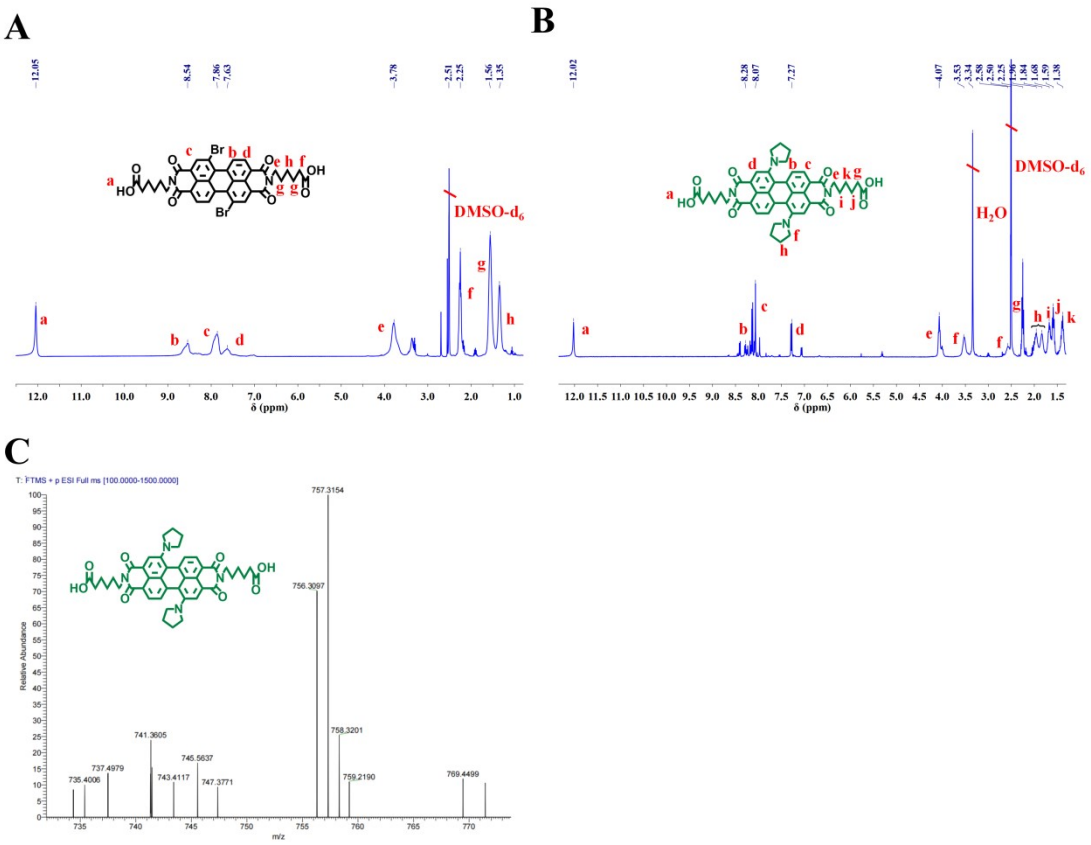


**Fig. S1** (A) $^{1}$H NMR spectrum of HOOC-PDI-COOH in DMSO-$d_6$. (B) $^{1}$H NMR spectrum of PDI0 in DMSO-$d_6$. (C) MS spectrum of PDI0 in acetonitrile (chromatographically pure).

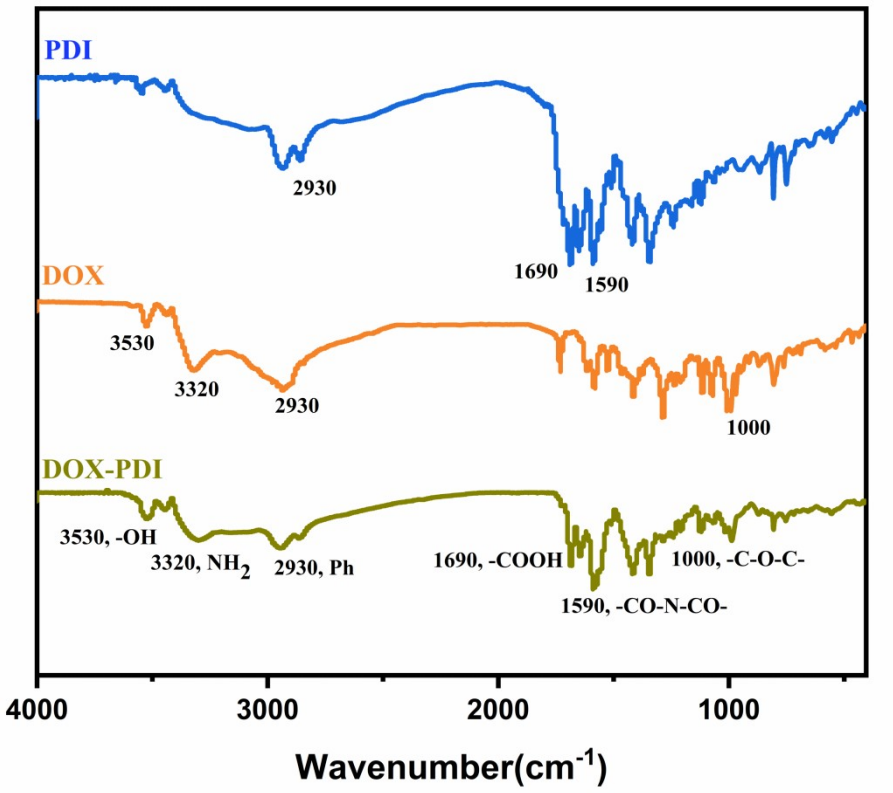


**Fig. S2** FT-IR spectra of free drugs (DOX, PDI0) and prepared DP NPs.

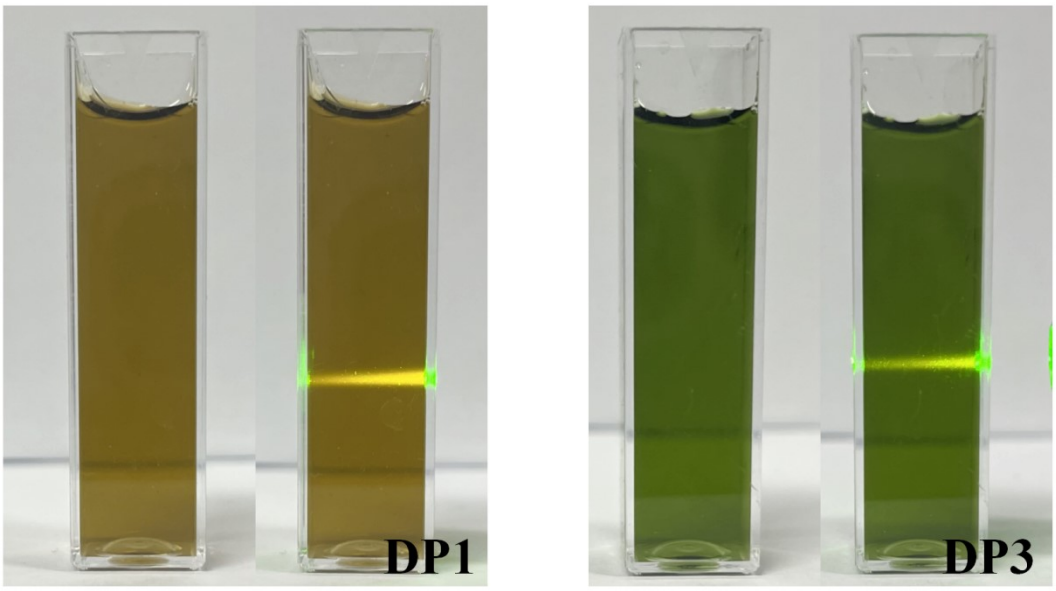


**Fig. S3** Tyndall effect of DP1 and DP3.

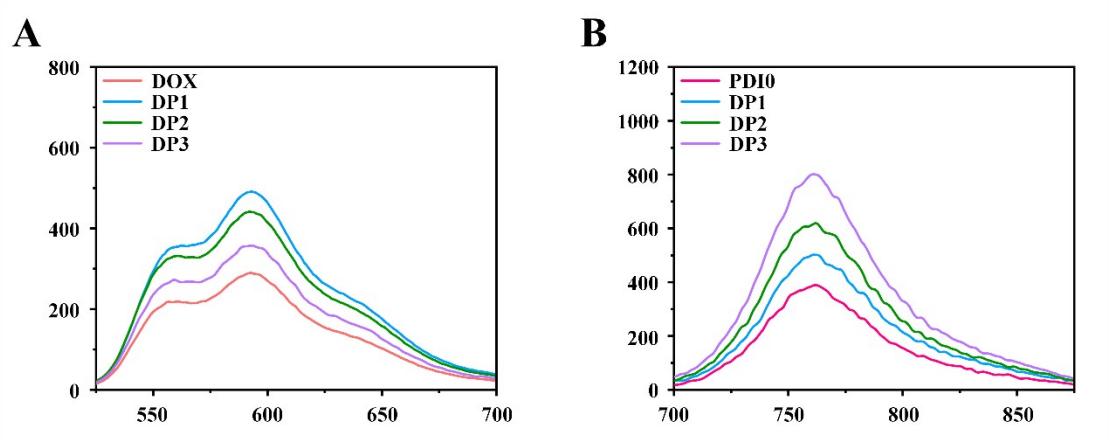


**Fig. S4** (A) Fluorescence spectra of free DOX and DP NPs in deionized water. (B) Fluorescence spectra of free PDI0 and DP NPs in deionized water.

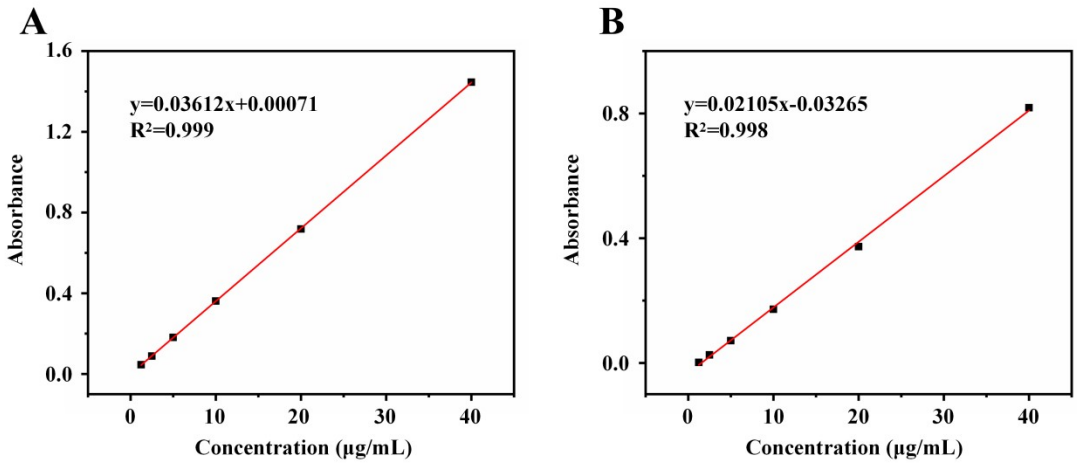


**Fig. S5** The standard curves of PDI0 (A) and DOX (B) in DMSO.

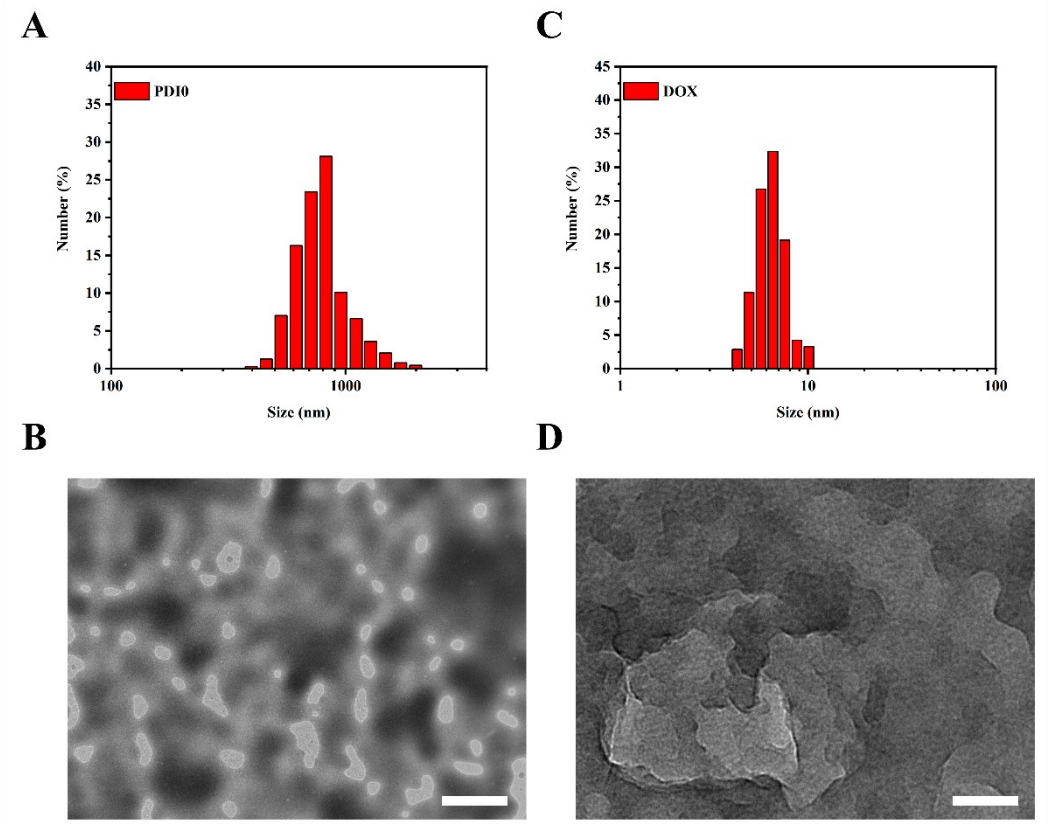


**Fig. S6** DLS (A) and TEM (B) of free PDI0; DLS (C) and TEM (D) of free DOX (Scale bar: 1μm).

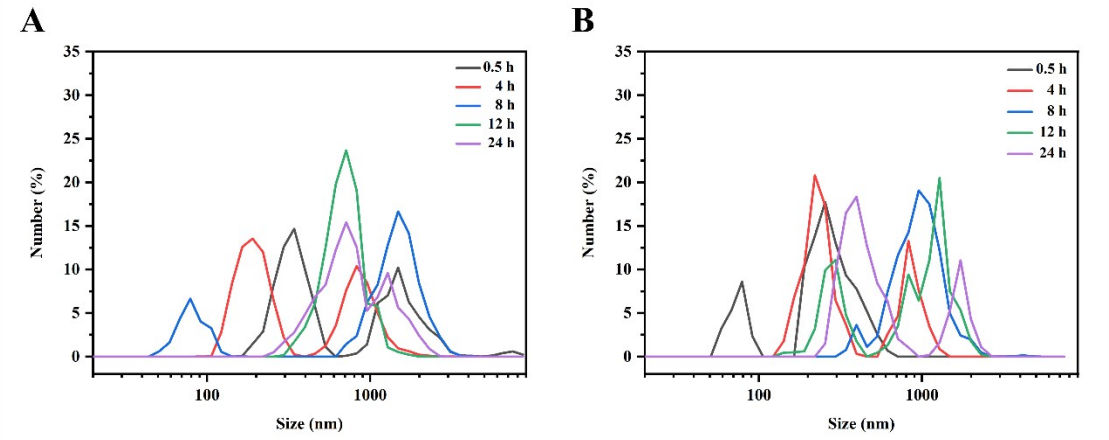


**Fig. S7** The hydrodynamic diameter of DP1 (A) and DP3 (B) in pH 5.0.

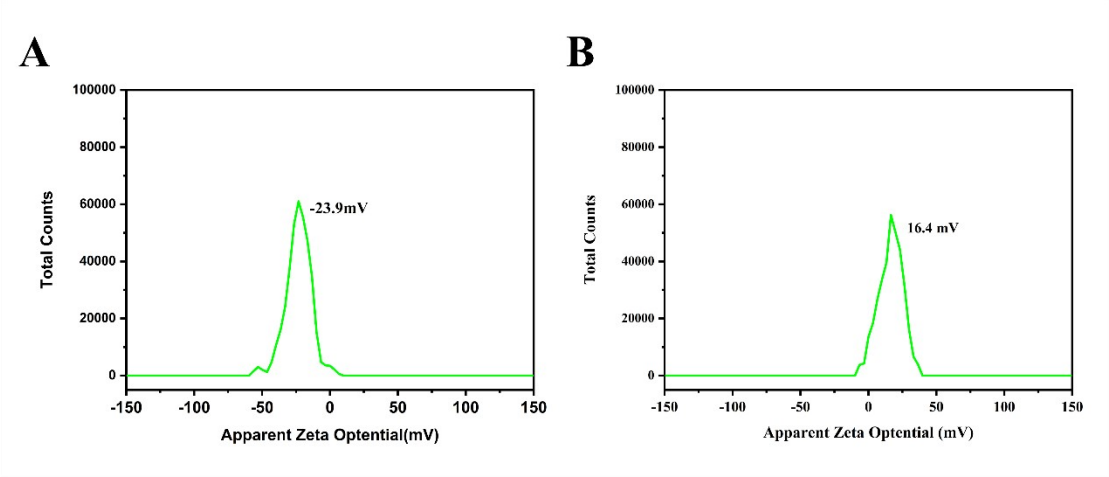


**Fig. S8** Zeta potential measurement of DP2 in PBS (pH 7.4) (A) and in PBS (pH 5.0) (B).

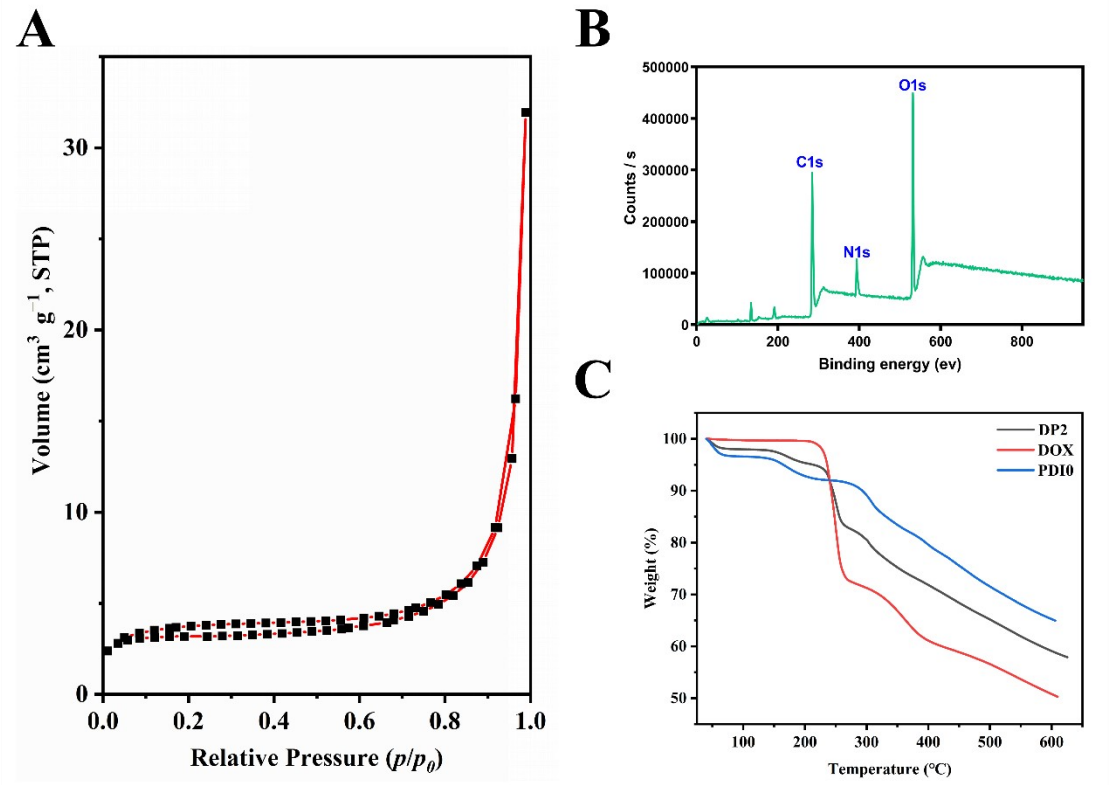


**Fig. S9** (A) $N_2$ adsorption – desorption isotherms of DP2, (B) XPS spectrum of DP2, (C) TGA thermograms.

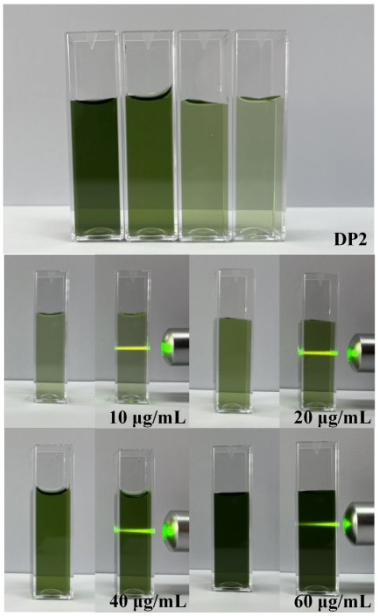


**Fig. S10** Photographs and Tyndall effect of DP2 at different concentrations.

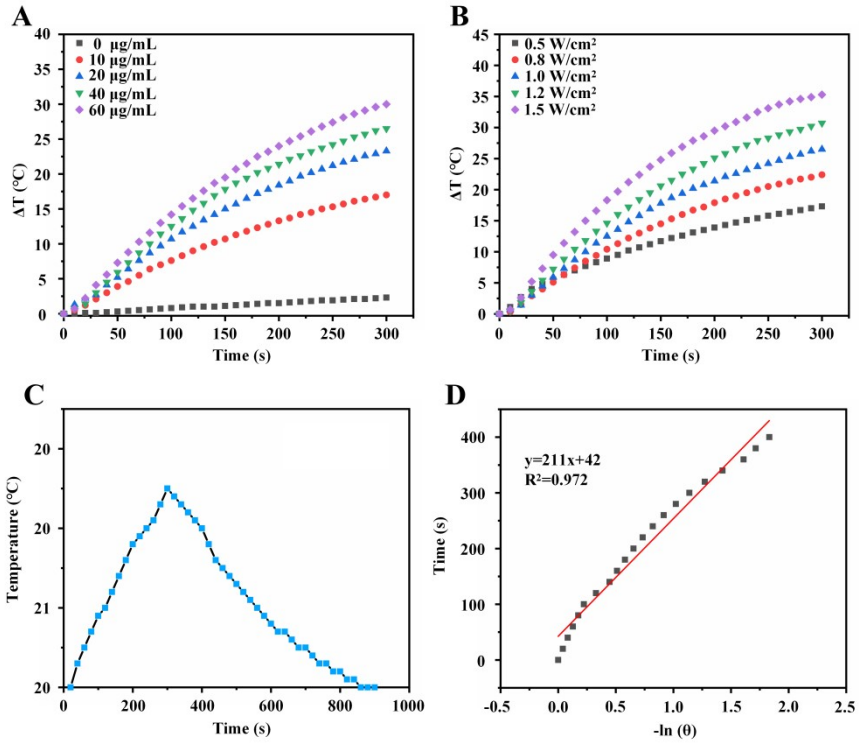


**Fig. S11** (A) Photothermal effect of free PDI0 at different concentrations with 660 nm laser irradiation (1 W/cm$^2$). (B) Photothermal heating curves of free PDI0 under different laser power densities. (C) Photothermal heating and cooling curves of water. (D) The relationship of negative natural logarithm of θ and cooling time of water.

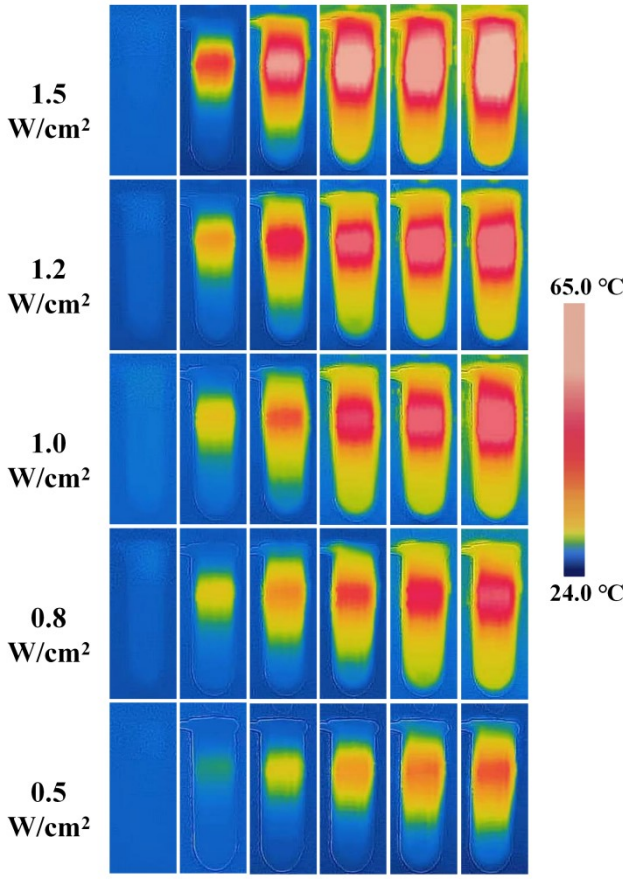


**Fig. S12** The infrared thermal images of DP2 irradiated with 660 nm laser under different power densities.

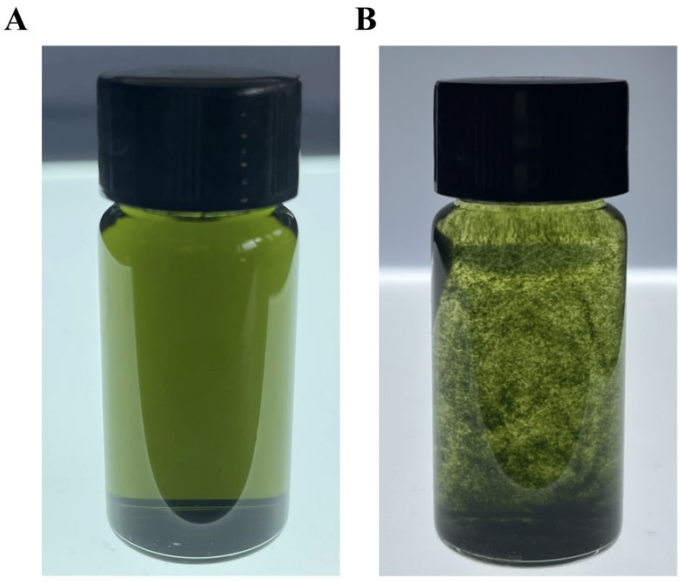


**Fig. S13** Photographs of PDI0 under different pH, (A) 7.4 and (B) 5.0.

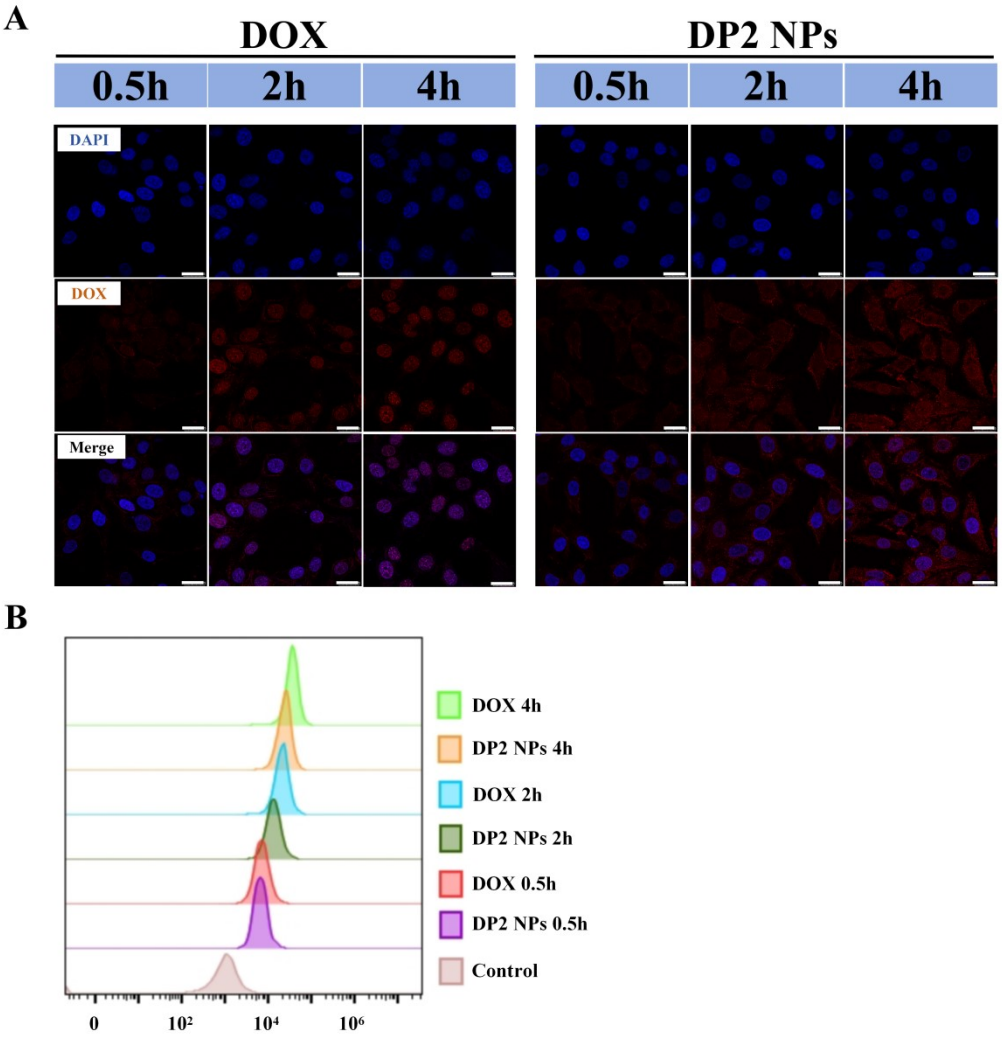


**Fig. S14** (A) CLSM images of HepG 2 cells incubated with free DOX and DP2 for 0.5, 2 and 4 h (scale bar: 25 μm). (B) Flow cytometry (FCM) analysis of HepG 2 cells after incubation with free DOX and DP2.

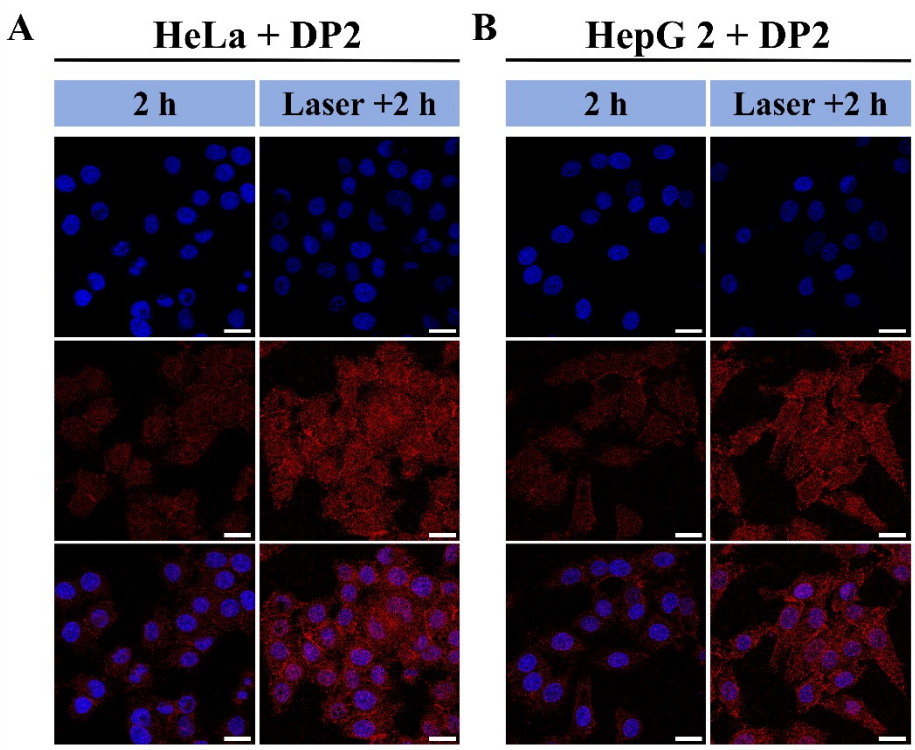


**Fig. S15** CLSM images of HeLa and HepG 2 cells incubated with DP2 in the presence or absence of 660 nm laser for 2 h (scale bar: 25 μm).

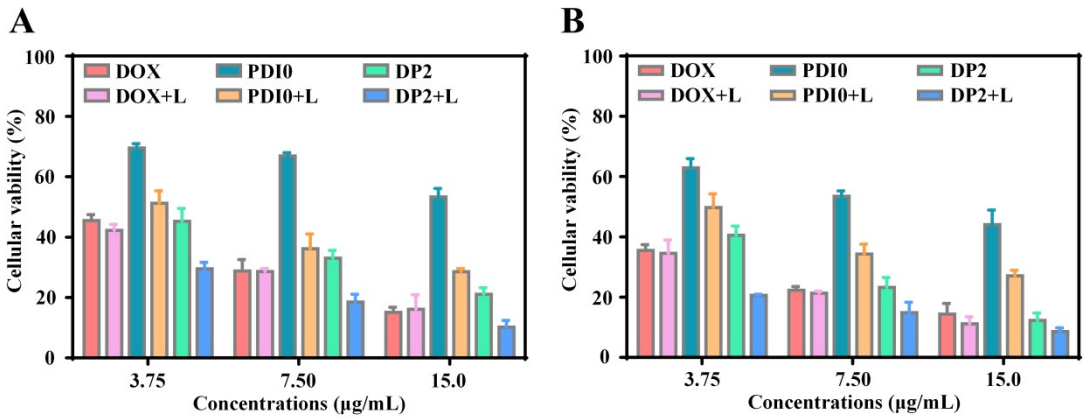


**Fig. S16** Cell viability of HepG 2 cells incubated with DOX, DOX + Laser, PDI0, PDI0 + Laser, DP2, and DP2 + Laser at different concentrations for 24 h (A) and 48 h (B).

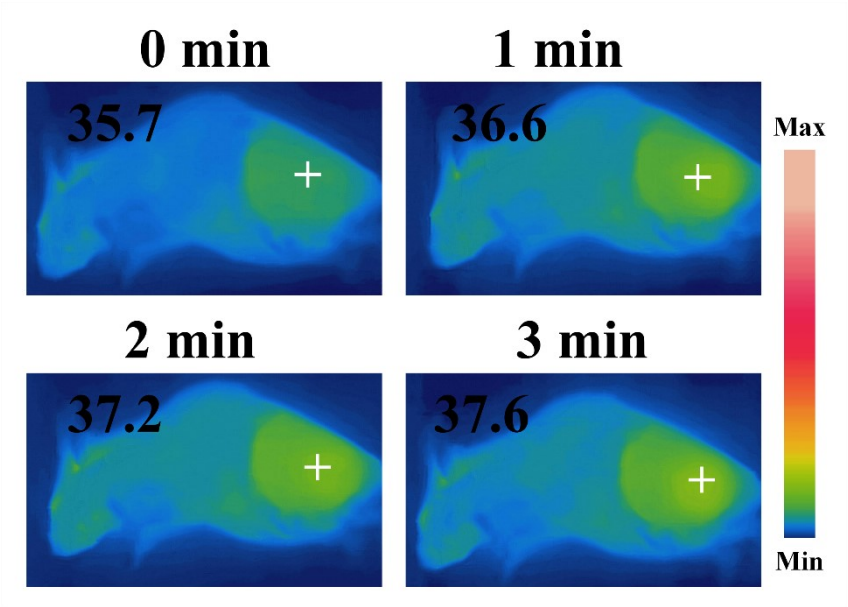


**Fig. S17** The photothermal images of 4T1 tumor-bearing mice after injection of PBS.

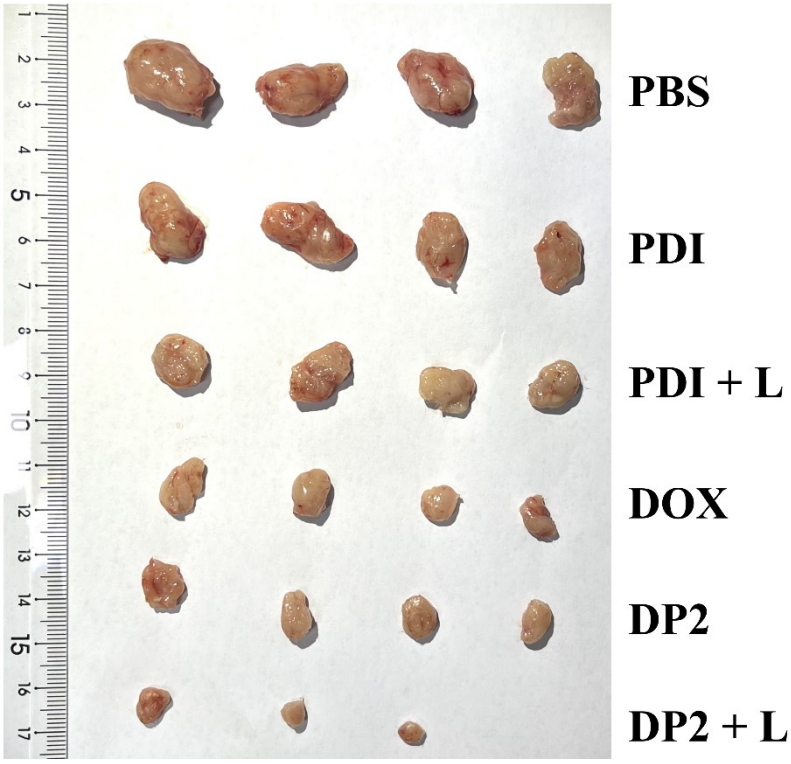


**Fig. S18** Photograph of 4T1 tumors harvested at day 14 after different treatments.

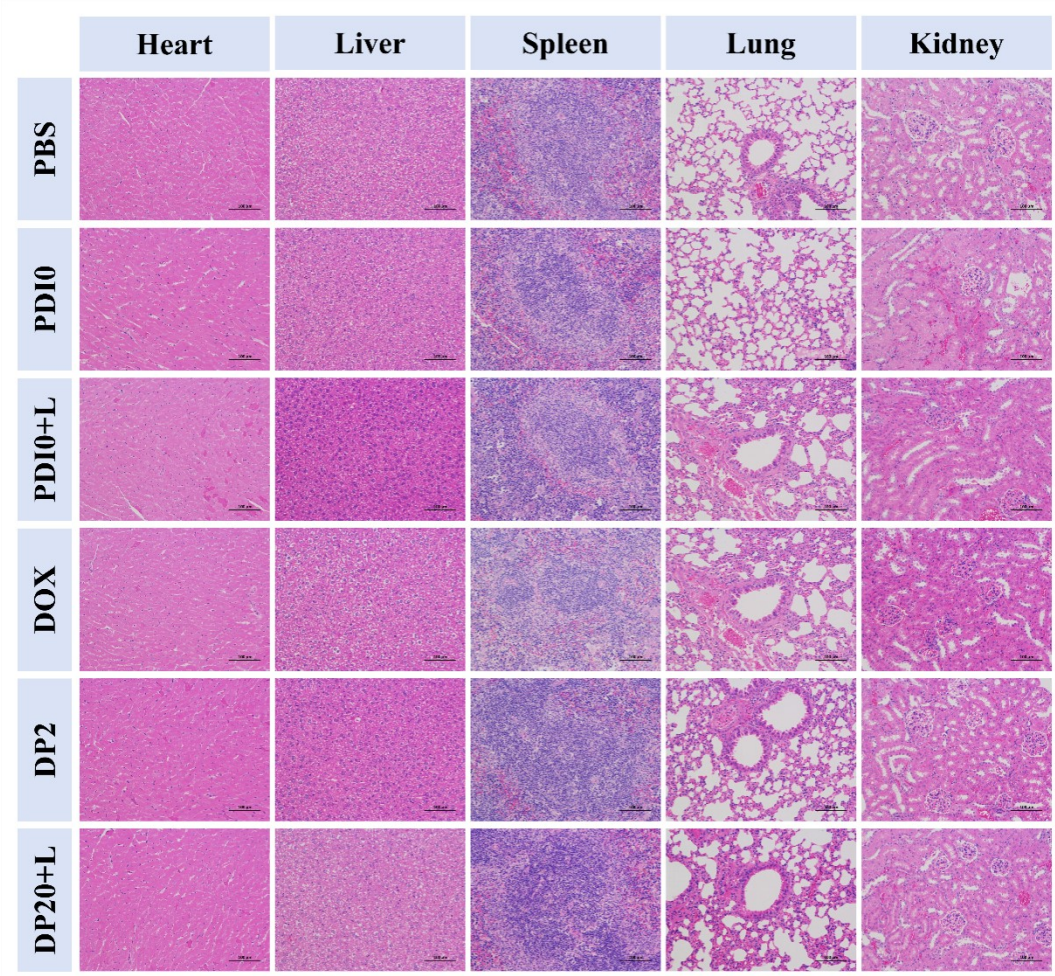


**Fig. S19** H&E staining of heart, liver, spleen, lung and kidney from different treatment groups (Scale bar: 100 μm).

## Reference

1. J. Li, C. Liu, Y. Hu, C. Ji, S. Li and M. Yin, *Theranostics*, 2020, **10**, 166-178.